

Transition-Metal Ions in Zeolites: Coordination and Activation of Oxygen

Pieter J. Smeets,^{†,‡} Julia S. Woertink,[‡] Bert F. Sels,[†] Edward I. Solomon,^{‡,§} and Robert A. Schoonheydt[†]

[†]Center for Surface Chemistry and Catalysis, KU Leuven, Kasteelpark Arenberg 23, 3001 Leuven, Belgium, [‡]Department of Chemistry, Stanford University, Stanford, California 94305, and

[§]Stanford Synchrotron Radiation Lab, Menlo Park, California 94025

Received September 11, 2009

Zeolites containing transition-metal ions (TMIs) often show promising activity as heterogeneous catalysts in pollution abatement and selective oxidation reactions. In this paper, two aspects of research on the TMIs Cu, Co, and Fe in zeolites are discussed: (i) coordination to the lattice and (ii) activated oxygen species. At low loading, TMIs preferably occupy exchange sites in six-membered oxygen rings (6MR), where the TMIs preferentially coordinate with the O atoms of Al tetrahedra. High TMI loadings result in a variety of TMI species formed at the zeolite surface. Removal of the extralattice O atoms during high-temperature pretreatments can result in autoreduction. Oxidation of reduced TMI sites often results in the formation of highly reactive oxygen species. In Cu-ZSM-5, calcination with O₂ results in the formation of a species, which was found to be a crucial intermediate in both the direct decomposition of NO and N₂O and the selective oxidation of methane into methanol. An activated oxygen species, called α-O, is formed in Fe-ZSM5 and reported to be the active site in the partial oxidation of methane and benzene into methanol and phenol, respectively. However, this reactive α-O can only be formed with N₂O, not with O₂. O₂-activated Co intermediates in faujasite (FAU) zeolites can selectively oxidize α-pinene and epoxidize styrene. In Co-FAU, Co^{III} superoxo and peroxy complexes are suggested to be the active cores, whereas in Cu and Fe-ZSM-5, various monomeric and dimeric sites have been proposed, but no consensus has been obtained. Very recently, the active site in Cu-ZSM-5 was identified as a bent [Cu–O–Cu]²⁺ core (*Proc. Natl. Acad. Sci. U.S.A.* **2009**, *106*, 18908–18913). Overall, O₂ activation depends on the interplay of structural factors such as the type of zeolite and sizes of the channels and cages and chemical factors such as the Si/Al ratio and the nature, charge, and distribution of the charge-balancing cations. The presence of several different TMI sites hinders the direct study of the spectroscopic features of the active site. Spectroscopic techniques capable of selectively probing these sites, even if they only constitute a minor fraction of the total amount of TMI sites, are thus required. Fundamental knowledge of the geometric and electronic structures of the reactive active site can help in the design of novel selective oxidation catalysts.

1. Introduction

The interaction of O₂ with the surface atoms in the micropores and channels of zeolites has been studied since the 1960s. It was recognized at that time that the adsorption enthalpy of N₂ in zeolite A [Linde type A zeolite (LTA); Figure 1A] was systematically higher than that of O₂ because of the quadrupolar moment of N₂. The pressure-swing-adsorption process was developed to separate O₂ and N₂

from air on an industrial scale.^{1–6} The adsorption enthalpy of O₂ at zero coverage is 15–20 kJ/mol. The adsorbed molecule is coordinated end-on to the exchangeable cations, thus making the infrared (IR)-inactive stretching vibration of O₂ active. The measured values range from 1555 to 1552 cm⁻¹ for alkali- and alkaline-earth-exchanged zeolites, slightly below the 1556 cm⁻¹ measured by Raman spectroscopy for gaseous O₂.^{7–9} However, for O₂ in interaction with Cu⁺ in faujasite (FAU), O=O stretching vibrations at 1256 and 1180 cm⁻¹ were recently measured.¹⁰ These were ascribed to O₂ interacting with Cu⁺ in sites II and III of the FAU framework, respectively (see Figure 1B). This red shift points to a

*To whom correspondence should be addressed. E-mail: robert.schoonheydt@biw.kuleuven.be. Tel.: +32-16-321610.

(1) Breck, D. W. *Zeolite Molecular Sieves*; Wiley & Sons: New York, 1974; p 771.
 (2) Shen, D. M.; Bulow, M.; Siperstein, F.; Engelhard, M.; Myers, A. L. *Adsorption* **2000**, *6*, 275–286.
 (3) McKee, D. W. U.S. Patent 3,140,933, **1964**.
 (4) Yang, R. T.; Chen, Y. D.; Peck, J. D.; Chen, N. *Ind. Eng. Chem. Res.* **1996**, *35*, 3093–3099.
 (5) Dunne, J. A.; Mariwals, R.; Rao, M.; Sircar, S.; Gorte, R. J.; Myers, A. L. *Langmuir* **1996**, *12*, 5888–5895.
 (6) Chao, C. C. Eur. Patent EP0297542A2, **1983**.

(7) Jousse, F.; DeLara, E. C. *J. Phys. Chem.* **1996**, *100*, 233–237.
 (8) Jousse, F.; Larin, A. V.; DeLara, E. C. *J. Phys. Chem.* **1996**, *100*, 238–244.
 (9) Xu, J.; Mojet, B. L.; van Ommen, J. G.; Lefferts, L. *J. Phys. Chem. B* **2005**, *109*, 18361–18368.
 (10) Santra, S.; Archipov, T. E.; Augusta B.; Komnik, H.; Stoll, H.; Roduner, E.; Rauhut, G. *Phys. Chem. Chem. Phys.* **2009**, DOI: 10.1039/b904152d.

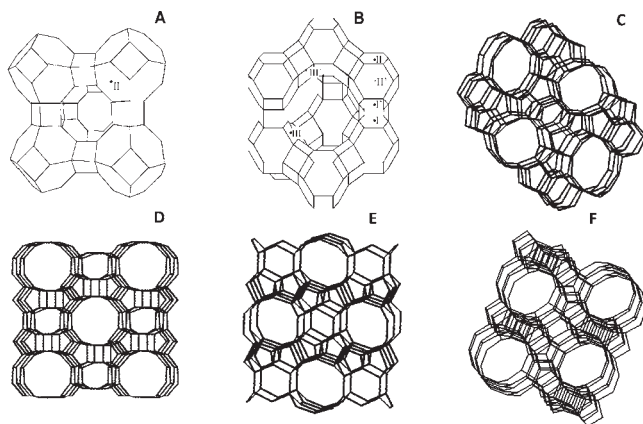
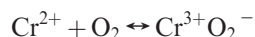


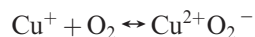
Figure 1. Industrially most important zeolite structures: (A) LTA, (B) X, and Y (FAU topology); (C) ZSM-5 (MFI topology); (D) MOR, (E) FER, and (F) *BEA. The symbols I, I', II, II', III, and III' indicate exchangeable cation sites in LTA and FAU. The lines represent the O atoms and the corners Si or Al atoms. ZSM-5, MOR, and FER are also known as pentasil zeolites.

significant weakening of the O=O bond due to electron transfer from Cu^+ to the π^* -antibonding orbitals of O_2 .

Such an electron transfer was already observed in the 1970s by Klier and co-workers in zeolite A loaded with transition-metal ion (TMI).^{11–14} Thus, Cr^{II} A reversibly adsorbs one O_2 per Cr^{II} at room temperature. The spectral changes point to the reaction



and similarly for Cu^+



Fe^{2+} in zeolite A does not bind O_2 at room temperature, but upon heating in O_2 , Fe^{2+} is oxidized to Fe^{3+} , and the formation of a $\text{Fe}^{3+}\text{—O—Fe}^{3+}$ species was suggested.¹⁴

At about the same time, Lunsford and co-workers prepared FAU-type zeolites (Figure 1B) loaded with amine complexes of Cu^{2+} and Co^{2+} .^{15,16} The cobaltamine complexes take up

O_2 at room temperature to form the corresponding mononuclear superoxo complexes, identified by their characteristic UV–vis and electron paramagnetic resonance (EPR) spectra. These mononuclear superoxo complexes were unstable because of their mobility in the zeolitic cavities and evolved slowly into dinuclear peroxo complexes.^{17,18} Later on, bulky Co complexes were synthesized in the supercages of zeolite Y. These complexes were trapped in the supercages and could not diffuse through the zeolitic cavity system. Upon interaction with O_2 , stable mononuclear superoxo complexes were obtained.¹⁸

In the search for new and improved heterogeneous catalysts for pollution abatement and selective oxidation, research was redirected to TMI in mordenite (MOR) and MFI-type zeolites (Figure 1C,D), with ZSM-5 (a zeolite with MFI topology) as the most prominent example. In this paper, we discuss the activation of O_2 by TMI in these zeolite topologies, with special emphasis on the selective oxidation of hydrocarbons and catalytic decomposition of N_2O and NO into N_2 and O_2 . After a short introduction on the fundamentals of zeolite structures, this contribution presents an overview of the present state of knowledge of the coordination of TMI with surface oxygen. Several excellent reviews have been published on the catalytic oxidation of organic substrates by TMI in zeolites or on other supports.^{19–24} In this paper, we will focus mainly on the first-row TMIs Cu, Fe, and Co in zeolites. Because some of these coordinated TMIs are able to activate O_2 or N_2O under moderate conditions, understanding their geometric and electronic structures might lead to the development of novel active and selective oxidation catalysts.

2. Zeolites

Zeolites are three-dimensional microporous silicates. The primary building unit is the $[\text{SiO}_4]^{4-}$ tetrahedron. It forms a three-dimensional network through corner-sharing of the four O atoms and leads to a charge-neutral network.^{1,25} Because of crystalline ordering, zeolites contain ordered pores and cavities that have characteristic shapes and sizes. A total of 176 different structure types are known.²⁶ Some of these can be found in nature as minerals, but most are synthetic materials. Corner-sharing and strictly alternating negatively charged Al and positively charged P tetrahedra, $[\text{AlO}_4]^{5-}$ and $[\text{PO}_4]^{3-}$, can also be used as primary tetrahedral units. They give the so-called crystalline, microporous AIPO materials. Some of them are isostructural with the silicates, and others do not have a siliceous counterpart. Zeolites are represented with three-letter codes, which are under the supervision of the structure commission of the International Zeolite Association (IZA).^{26,27}

Isomorphous substitution is the replacement of a cation in the lattice by another cation with approximately the same size but with different charge. The most important is the substitution of Si^{4+} by Al^{3+} , thus giving an overall negative charge to the framework. This charge is neutralized by exchangeable cations, located in the channels or cages of the structure. The amount of exchangeable cations is expressed by the cation exchange capacity. In principle, the degree of Al for Si substitution ranges from zero ($\text{Si}/\text{Al} = \text{infinity}$) to $\text{Si}/\text{Al} = 1$. Whatever the Si/Al ratio, the isomorphous substitution obeys Loewenstein's rule: two Al

(19) De Vos, D. E.; Dams, M.; Sels, B. F.; Jacobs, P. A. *Chem. Rev.* **2002**, *102*, 3615–3640.

(20) Corma, A.; Garcia, H. *Chem. Rev.* **2002**, *102*, 3837–3892.

(21) Ratnasamy, P.; Srinivas, D. *Catal. Today* **2009**, *141*, 3–11.

(22) Corma, A. *Chem. Rev.* **1997**, *97*, 2373–2419.

(23) Punniyamurthy, T.; Velusamy, S.; Iqbal, J. *Chem. Rev.* **2005**, *105*, 2329–2363.

(24) Viswanathan, B.; Jacob, B. *Catal. Rev.* **2005**, *47*, 1–82.

(25) van Bekkum, H.; Flanigen, E.; Jacobs, P. A.; Jansen, J. C. *Introduction to Zeolite Science and Practice*, 2nd ed.; Elsevier: Amsterdam, The Netherlands, 2001; p 1018.

(26) Baerlocher, C.; McCusker, L. B. Database of Zeolite Structures. <http://www.iza-structure.org/databases/>.

(27) Treacy, M. M. J.; Higgins, J. B. *Collection of Simulated XRD Powder Patterns for Zeolites*, 5th ed.; Elsevier: Amsterdam, The Netherlands, 2007.

(11) Klier, K. *Langmuir* **1988**, *4*, 13–25.

(12) Kellerman, R.; Hutta, P. J.; Klier, K. *J. Am. Chem. Soc.* **1974**, *96*, 5946–5947.

(13) Kellerman, R.; Klier, K. In *Molecular Sieves—II*; Katzer, J. R., Ed.; American Chemical Society: Washington, DC, 1977; Vol. 40, p 120.

(14) Lange, J. P.; Klier, K. *Zeolites* **1994**, *14*, 462–468.

(15) Vansant, E. F.; Lunsford, J. H. *J. Phys. Chem.* **1972**, *76*, 2860.

(16) Lunsford, J. *ACS Symp. Ser.* **1977**, *40*, 473.

(17) Schoonheydt, R. A.; Pelgrims, J. *J. Chem. Soc., Dalton Trans.* **1981**, 914–922.

(18) Devos, D. E.; Knops-Gerrits, P. P.; Parton, R. F.; Weckhuysen, B. M.; Jacobs, P. A.; Schoonheydt, R. A. *J. Inclusion Phenom. Mol. Recognit. Chem.* **1995**, *21*, 185–213.

Table 1. Pore Sizes, Typical Unit Cell Compositions, and Dimensionality of the Channel Systems of LTA, FAU MFI, MOR, FER, and *BEA²⁶

zeolite topology	pore size (Å)	unit cell	channel system
LTA	8-ring: 4.1 × 4.1	$[\text{Na}^+_{12}(\text{H}_2\text{O})_m][\text{Al}_{12}\text{Si}_{12}\text{O}_{48}]$	three-dimensional
FAU	12-ring: 7.4 × 7.4	$[(\text{Ca}^{2+}\text{Mg}^{2+}\text{Na}^+_{29})(\text{H}_2\text{O})_m][\text{Al}_{58}\text{Si}_{134}\text{O}_{384}]$	three-dimensional
MFI	10-ring: 5.1 × 5.5 10-ring: 5.3 × 5.6	$[\text{Na}^+_n(\text{H}_2\text{O})_m][\text{Al}_n\text{Si}_{96-n}\text{O}_{192}]$	two-dimensional
MOR	12-ring: 6.5 × 7.0 8-ring: 2.6 × 5.7	$[\text{Na}^+_8(\text{H}_2\text{O})_m][\text{Al}_8\text{Si}_{40}\text{O}_{96}]$	one-dimensional
FER	10-ring: 4.2 × 5.4 8-ring: 3.5 × 4.8	$[\text{Mg}^{2+}_2\text{Na}^+_{29}(\text{H}_2\text{O})_m][\text{Al}_6\text{Si}_{30}\text{O}_{72}]$	two-dimensional
*BEA	12-ring: 6.6 × 6.7 12-ring: 5.6 × 5.6	$[\text{Na}^+_{77}(\text{H}_2\text{O})_m][\text{Al}_7\text{Si}_{57}\text{O}_{128}]$	three-dimensional

tetrahedra cannot be neighbors sharing an O atom.¹ Thus, an Al tetrahedron must share its four O atoms with four Si tetrahedra, and with Si/Al = 1, a strict alternation of Si and Al tetrahedra occurs in the structure. Such is the case for zeolite A (LTA).

In industrial applications, the most important zeolites are LTA, FAU, MFI, and MOR. Their idealized structures are shown in Figure 1. Table 1 summarizes their unit cell dimensions and typical sizes of their channels/cages. The dimensions of the zeolite pores allow for the separation of molecules on the basis of their sizes, the so-called molecular sieving effect. In catalysis, this property is often referred to as shape selectivity.²⁵ An example is the cracking of alkanes in acid MFI-type zeolites. Here the zeolite pores allow only the linear molecules to enter the pores containing the acid sites that regulate the cracking. Branched molecules are excluded from the pores and hence do not react.²⁸

Another area of zeolite research is the immobilization of homogeneous catalysts. In FAU zeolites, for instance, TMI complexes exchanged in the supercages are readily accessible for reagents [unlike the TMI exchanged in the sodalite cages,²⁹ which are only accessible through a six-membered oxygen ring (6MR)]. After the reaction, a simple filtration suffices to separate the catalyst from the reaction products. This separation is often problematic in the case of homogeneous catalysts. As an example, superoxo and peroxy complexes have been obtained in the supercages of zeolite Y by interaction of O₂ with cobaltamine complexes, immobilized in the supercages of zeolite Y.¹⁸ There are several ways to synthesize these complexes in the supercages, with the preferred procedure depending on the type of complex. If the complexes are stable under exchange conditions, cationic, and smaller than the free diameter of the 12-membered ring (MR) giving access to the supercages, they can be exchanged from aqueous solution. Other syntheses involve the adsorption of appropriate ligands in the zeolite, preexchanged with TMI, or the complexes can be synthesized in situ, e.g., in the supercages of FAU-type zeolites.^{18,19,30}

TMI can, in principle, substitute for Si⁴⁺ or Al³⁺ in the zeolitic structures during synthesis, resulting in a zeolite lattice containing TMI. Parameters to be taken into account are (i) the size and charge of the TMI, (ii) the pH of the synthesis medium, and (iii) the ability of the TMI to adopt tetrahedral coordination with O atoms. In most cases, the

amount of TMI incorporated in the lattice by hydrothermal synthesis is very limited. The two most common examples are Ti⁴⁺ and Fe³⁺. Ti⁴⁺ exchanged in silicalite, for instance, is called TS-1 and is found to be an active catalyst in converting benzene with hydrogen peroxide into phenol.^{31–33} Fe³⁺ in the lattice is often due to the presence of an impurity in the zeolite synthesis, but it can also be added as a reagent into the synthesis mixture. One of the problems with TMI in the lattice is thermal stability. Upon high-temperature treatment, some of the TMIs in the structure are extracted and found as so-called extralattice TMIs, which can be monomeric or dimeric or appear as oligomers.³⁴ All of them are possible catalytic sites.

Aqueous ion exchange is the most commonly used method for preparing zeolites with TMIs located at exchange sites. The resulting material contains aqueous TMIs in the pores and cavities of the zeolite. Upon high-temperature treatment, water is removed and the TMIs coordinate to the surface oxygens of the exchange sites. These sites had been compiled by Mortier a long time ago.³⁵ They are crystallographically well-defined in the case of zeolites with low Si/Al ratios such as LTA, FAU, and MOR (Figure 1). This is much less so for zeolites with high Si/Al ratios such as MFI.

Because aqueous solutions of TMI can be acidic, the exchange reaction can be accompanied by side reactions such as the exchange of protons and partial lattice destruction. To avoid these side effects, other exchange techniques have been developed, including solid-state exchange^{36–38} or simple buffering of the aqueous solution.^{39,40}

3. Coordination of TMI in Zeolite Channels and Cages

As mentioned above, isomorphous substitution of Al³⁺ for Si⁴⁺ renders the zeolite framework negatively charged. This

(31) Notari, B. Innovation in Zeolite Materials Science. In *Studies in Surface Science and Catalysis*; Grobet, P. J., Mortier, W. J., Vansant, E. F., Schulz-Ekloff, G., Eds.; Elsevier: Amsterdam, The Netherlands, 1988; Vol. 37, p 413.

(32) Clerici, M. G.; Romano, U. Eur. Patent EP100119A1, 1983.

(33) Bellusi, G.; Giusti, A.; Esposito, A.; Buonomo, F. Eur. Patent EP226257A2, 1987.

(34) Pirngruber, G. The fascinating chemistry of iron- and copper-containing zeolites. In *Ordered Porous Materials*; Valtchev, V., Mintova, S., Tsapatsis, M., Eds.; Elsevier: Amsterdam, The Netherlands, 2008; p 733.

(35) Mortier, W. J. *Compilation of extra framework sites in zeolites*; Butterworth Sci. Ltd.: Guildford, U.K., 1982; p 67.

(36) Karge, H. G.; Zhang, Y.; Beyer, H. K. *Catal. Lett.* **1992**, *12*, 147–156.

(37) Weitkamp, J.; Ernst, S.; Bock, T.; Kromminga, T.; Kiss, A.; Kleinschmit, P. U.S. Patent 5,545,784, 1994.

(38) Sulikowski, B.; Find, J.; Karge, H. G.; Herein, D. *Zeolites* **1997**, *19*, 395–403.

(39) Iwamoto, M.; Yahiro, H.; Mine, Y.; Kagawa, S. *Chem. Lett.* **1989**, 213–216.

(40) Smeets, P. J.; Meng, Q. G.; Corthals, S.; Leeman, H.; Schoonheydt, R. A. *Appl. Catal., B* **2008**, *84*, 505–513.

(28) Jacobs, P. A.; Martens, J. A.; H. van Bekkum, E. M. F.; Jansen, J. C. Introduction to Acid Catalysis with Zeolites in Hydrocarbon Reactions. *Studies in Surface Science and Catalysis*; Elsevier: Amsterdam, The Netherlands, 1991; Vol. 58, pp 445–496.

(29) Smeets, P. J.; Sels, B. F.; van Teeffelen, R. M.; Leeman, H.; Hensen, E. J. M.; Schoonheydt, R. A. *J. Catal.* **2008**, *256*, 183–191.

(30) De Vos, D. E.; Sels, B. F.; Jacobs, P. A. *Adv. Catal.* **2001**, *46*, 1–87.

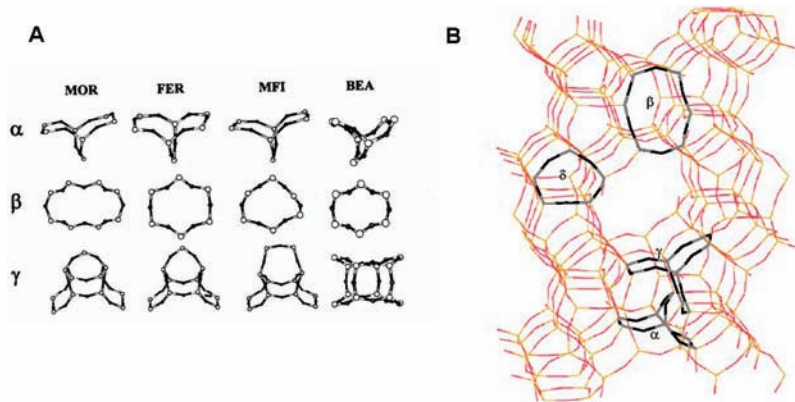


Figure 2. (A) Local framework structures of the α , β , and γ sites in the MOR, FER, MFI, and *BEA zeolites.⁴¹ (B) Crystallographic positions of these sites in ZSM-5.⁴⁹ Reproduced with permission from the PCCP Owner Societies 2003.

Table 2. d–d Transitions of Co^{2+} Occupying α , β , and γ Sites in the Pentasil Zeolites and *BEA^{42–44,46}

zeolite	energy (cm^{-1})		
	site α	site β	site γ
MFI	15 100	16 000, 17 150, 18 600, 21 200	20 100, 22 000
MOR	14 800	15 900, 17 500, 19 200, 21 100	20 150, 22 050
FER	15 000	16 000, 17 100, 18 700, 20 600	20 300, 22 000
*BEA	14 600	15 500, 16 300, 17 570, 21 700	18 900, 22 060

negative charge is compensated for by extraframework cations located in the pores or cages of the zeolite. Because these cations are not part of the framework, they can be exchanged by other cations, in particular TMI. The actual location depends on several factors, among which are the Si/Al ratio, the total amount of TMI, the charge of the TMI, the exchange method, and the conditions (with the pH and temperature being the most important).

Initially, the TMIs will occupy the most favorable exchange sites and try to maximize their coordination number. In FAU for instance, after dehydration, the TMIs are preferably located inside the hexagonal prisms (sites I; Figure 1B) and in the sodalite cages (sites I'; Figure 1B). At higher loadings, the more accessible exchange sites in the supercages [accessible through 12-membered oxygen rings (12MR)] are occupied (sites II and III; Figure 1B). Among these sites, sites I' and II are the most important. Both are 6MR. In MFI, TMIs are located in the 10-membered-ring (10MR) channels or at channel intersections. They are coordinated to 6MR containing one or two Al tetrahedra, but 5MR with one Al cannot be excluded. The same holds for MOR with its 12MR and 8MR channel systems.³⁵

TMIs coordinated to the zeolite lattice have typical spectroscopic signatures, i.e., d–d transitions and EPR spectra. These spectra are usually reasonably resolved at low loadings

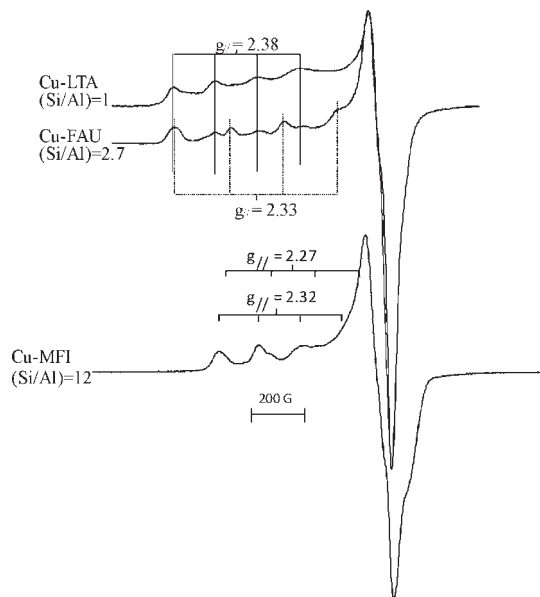


Figure 3. Typical EPR spectra of Cu^{2+} -LTA, Cu^{2+} -FAU, and Cu^{2+} -MFI after dehydration in O_2 at 450 °C.

of TMIs. In the work of Wichterlova and co-workers,^{41–46} three exchange sites are discerned for Co ions in pentasil zeolites and Beta (*BEA), denoted as α , β , and γ sites. In Figure 2A, an overview of these sites is shown, and their location in ZSM-5 is given in Figure 2B. Co^{2+} exchanged into one of these sites results in a characteristic set of d–d transitions in the UV–vis spectrum, as shown in Table 2. Using chemometric techniques, Verberckmoes et al. identified three different types of coordination sites for Co^{2+} in LTA and FAU zeolites from their ligand-field absorption spectrum: trigonal and pseudotetrahedral sites in site I', II, and II' and a pseudooctahedral site in site I (only in FAU; Figure 1).^{47,48}

(41) Wichterlova, B.; Dedecek, J.; Sobalik, Z. *NATO Sci. Ser., II* **2001**, *13*, 31–53.

(42) Dedecek, J.; Wichterlova, B. *J. Phys. Chem. B* **1999**, *103*, 1462–1476.

(43) Kaucky, D.; Dedecek, J. I.; Wichterlova, B. *Microporous Mesoporous Mater.* **1999**, *31*, 75–87.

(44) Dedecek, J.; Kaucky, D.; Wichterlova, B. *Microporous Mesoporous Mater.* **2000**, *35–36*, 483–494.

(45) Dedecek, J.; Kaucky, D.; Wichterlova, B.; Gonsiorova, O. *Phys. Chem. Chem. Phys.* **2002**, *4*, 5406–5413.

(46) Drozdova, L.; Prins, R.; Dedecek, J.; Sobalik, Z.; Wichterlova, B. *J. Phys. Chem. B* **2002**, *106*, 2240–2248.

(47) Verberckmoes, A. A.; Weckhuysen, B. M.; Pelgrims, J.; Schoonheydt, R. A. *J. Phys. Chem.* **1995**, *99*, 15222–15228.

(48) Verberckmoes, A. A.; Weckhuysen, B. M.; Schoonheydt, R. A. *Microporous Mesoporous Mater.* **1998**, *22*, 165–178.

(49) Groothaert, M. H.; Pierloot, K.; Delabie, A.; Schoonheydt, R. A. *Phys. Chem. Chem. Phys.* **2003**, *5*, 2135–2144.

Table 3. d–d Transitions and EPR Parameters of Cu²⁺ Coordinated to 6MRs in Zeolites after Dehydration (O₂ at 450 °C)^{54,59}

zeolite	d–d transitions (cm ⁻¹)	g	A × 10 ⁻⁴ cm ⁻¹	g _⊥	A _⊥ × 10 ⁻⁴ cm ⁻¹
LTA	10 500, 12 200, 15 100	2.37–2.41	130–145	2.06–2.07	19
FAU	10 300–10 700, 12 600, 15 000	2.36–2.41	120–145	2.06–2.08	19
		2.30–2.34	171–188	2.05–2.07	19
MOR, MFI	14 000 (broad)	2.30–2.33	156–180	2.04–2.07	3–25
		2.26–2.28	168–192	2.05–2.07	3–25

In the work of Schoonheydt and co-workers,^{49–54} a set of Cu-containing zeolites was studied with UV–vis–near-IR absorption and EPR spectroscopies. Examples of EPR spectra are shown in Figure 3, and the d–d transitions and EPR parameters of these Cu²⁺ sites are summarized in Table 3. For Cu²⁺ in FAU and LTA, three d–d transitions are resolved, with the most intense band in the region of 10 500–11 000 cm⁻¹ and two weaker bands around 12 500 and 15 000 cm⁻¹. The corresponding EPR spectra reveal two signals, one with g_{||} = 2.37–2.41 common for LTA and FAU and one with g_{||} = 2.30–2.34, not found in LTA. For MOR and MFI, the d–d transitions occur at higher energies and overlap such that only a broad band is observed at around 14 000 cm⁻¹. This d–d spectrum is accompanied by two EPR signals with characteristic g_{||} values of 2.30–2.33 and 2.26–2.28. The g_⊥ values are all situated in the 2.09–2.05 range, but the hyperfine splitting in the perpendicular region is not well resolved.

These spectra have traditionally been interpreted in terms of Cu²⁺ coordinating the 6MRs in a trigonal configuration (C_{3v}). The two EPR signals are then ascribed to 6MRs in different crystallographic positions, such as sites I' and II in FAU (Figure 1B), irrespective of the number of Al tetrahedra making up the 6MRs. A ligand-field analysis of the d–d transitions of Co²⁺ and Cu²⁺ in six-ring sites indicated that the TMIs are not symmetrically coordinated in the center of the ring but undergo an off-axial displacement.^{55–58} Detailed ab initio quantum-chemical analysis revealed that coordination of Cu²⁺ or Co²⁺ in a specific exchange site leads to a strong site distortion.^{49,51–54} First, the TMIs try to maximize their coordination number. Second, the O atoms of the Al tetrahedra are preferentially coordinated to the TMIs. This leads to site distortion, and the TMI is not located exactly in the center

of the 6MR. This is shown in Figure 4 for Cu²⁺ coordinated to lattice O atoms in the α, β, and γ sites in ZSM-5. This distortion depends on the number of Al tetrahedra making up the coordination site. Thus, a TMI in one crystallographic exchange site can have several spectroscopic signatures, depending on the number of Al tetrahedra. All of these studies taken together lead to the conclusion that both the crystallographic position of the exchange site and the number of Al tetrahedra making up the site determine the spectroscopic signatures of the TMIs in that site (see Figure 4).

At high TMI loading, additional less energetically favorable exchange sites are occupied, providing fewer coordination bonds to lattice O atoms. The spectroscopic signatures of TMIs in these sites are much less resolved because at high TMI loadings various TMI species can coexist: mono-, di-, and oligonuclear clusters up to chains of TMIs. Often the classical techniques used to characterize TMIs in zeolites, such as UV–vis absorption, EPR, X-ray diffraction, and extended X-ray absorption fine structure (EXAFS), give averages of overlaying spectra. At higher TMI loadings, some of the paramagnetic TMIs might be EPR-silent because of antiferromagnetic coupling and dipolar broadening, and subtle changes in the ligand field of TMIs at various sites result in the formation of overlapped unresolved absorption features. Further, EXAFS gives spectra that are a superposition from TMIs in different sites. Thus, it is extremely difficult to distinguish the contributions of a specific TMI site.

TMI sites can act as catalytic centers if they have open coordination sites and if they are readily accessible for guest molecules. In FAU zeolites, 6MRs separate the sodalite cages from the supercages, and as a result, the TMIs located inside the sodalite cages are inaccessible to molecules that cannot diffuse through the 6MR with a free diameter of ~0.23 nm. In MFI, TMIs are located in the straight or zigzag 10MR channels, which have a free diameter of ~0.55 nm. These are the only sites that can contribute to the overall catalytic activity. Similar considerations can be made for other zeolites: the smaller the pores, the less accessible the sites. In addition, larger pores allow for faster diffusion of reagents to the active sites inside the zeolite crystals and for the efficient release of reaction products out of the zeolite crystals, thereby (i) liberating the active site faster for a second reaction and (ii) decreasing the probability of unwanted side reactions, thus increasing the selectivity.

TMI-loaded zeolites such as Co³⁺, Fe³⁺, and Cu²⁺ can undergo auto-reduction during high-temperature pretreatment in He or under vacuum. The auto-reduction of Fe³⁺ to Fe²⁺ during He treatments is reported^{60–63} and confirmed

(50) Schoonheydt, R. A. *Catal. Rev.* **1993**, *35*, 129–168.(51) Pierloot, K.; Delabie, A.; Verberckmoes, A.; Schoonheydt, R. The Interplay between DFT and Conventional Quantum Chemistry: Coordination of Transition Metal Ions to Six-Rings in Zeolites. In *Density Functional Theory, a bridge between chemistry and physics*; Geerlings, P., De Proft, F., Langenaeker, W., Eds.; VUB University Press: Brussels, Belgium, 1999; p 169.(52) Pierloot, K.; Delabie, A.; Groothaert, M. H.; Schoonheydt, R. A. *Phys. Chem. Chem. Phys.* **2001**, *3*, 2174–2183.(53) Delabie, A.; Pierloot, K.; Groothaert, M. H.; Weckhuysen, B. M.; Schoonheydt, R. A. *Phys. Chem. Chem. Phys.* **2002**, *4*, 134–145.(54) Delabie, A.; Pierloot, K.; Groothaert, M. H.; Schoonheydt, R. A.; Vanquickenborne, L. G. *Eur. J. Inorg. Chem.* **2002**, 515–530.(55) Pierloot, K.; Delabie, A.; Ribbing, C.; Verberckmoes, A. A.; Schoonheydt, R. A. *J. Phys. Chem. B* **1998**, *102*, 10789–10798.(56) Verberckmoes, A.; Schoonheydt, R.; Ceulemans, A.; Delabie, A.; Pierloot, K. Semiempirical and ab-initio Calculations of the Spectroscopic properties of Co(II) coordinated in Zeolite A. In *Proceedings of the 12th International Zeolite Conference*; Treacy, M., Marcus, B., Bisher, M., Higgins, J., Eds.; Materials Research Society: Warrendale, PA, 1999; p 387.(57) Klier, K.; Dutta, P. J.; Kellerman, R. In *Molecular Sieves—II*; Katzer, J. R., Ed.; American Chemical Society: Washington, DC, 1977; Vol. 40, p 108.(58) Klier, K. Electronic structure of transition-metal ion containing zeolites. In *Catalysis by Unique Metal Structures in Solid Matrices—From Science to Applications*; Centi, G., Bell, A. T., Wichterlova, B., Eds.; Kluwer Academic Press: Dordrecht, The Netherlands, 2001; p 115.(59) Schoonheydt, R. A. *J. Phys. Chem. Solids* **1989**, *50*, 523–539.(60) Perez-Ramirez, J.; Mul, G.; Kapteijn, F.; Moulijn, J. A.; Overweg, A. R.; Domenech, A.; Ribera, A.; Arends, I. *J. Catal.* **2002**, *207*, 113–126.(61) Zecchina, A.; Rivallan, M.; Berlier, G.; Lamberti, C.; Ricchiardi, G. *Phys. Chem. Chem. Phys.* **2007**, *9*, 3483–3499.(62) Lobree, L. J.; Hwang, I. C.; Reimer, J. A.; Bell, A. T. *J. Catal.* **1999**, *186*, 242–253.(63) Joyner, R.; Stockenhuber, M. *J. Phys. Chem. B* **1999**, *103*, 5963–5976.

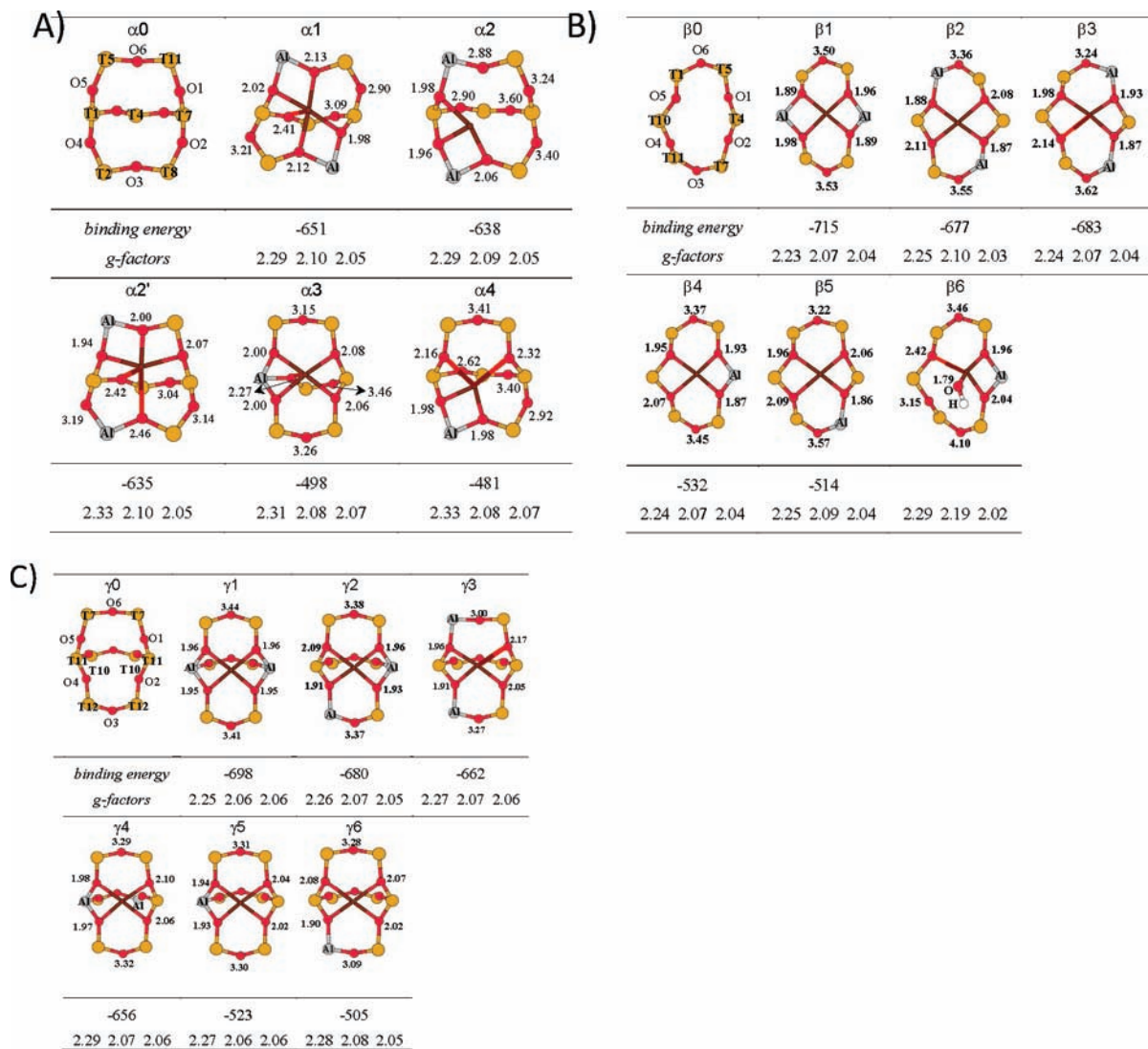


Figure 4. Optimized Cu^{II} coordination (brown) in the α (A), β (B), and γ (C) sites of ZSM-5 containing one or two lattice Al T sites. The corresponding Cu–O distances (Å), Cu^{II} binding energies (kcal/mol), and g factors of the distorted sites are given. The Cu^{II}-free sites are shown as $\alpha 0$, $\beta 0$, and $\gamma 0$.⁴⁹ Reproduced with permission from the PCCP Owner Societies 2003.

by L- and K-edge X-ray absorption spectroscopy measurements.^{64–67} It was attributed to the dehydration and desorption of O₂ from two Fe³⁺(OH)₂ sites, leaving two Fe²⁺(OH) species.^{62,68} In Cu zeolites, it has been reported that this autoreduction can be achieved by the dehydration of two Cu²⁺(OH) sites, resulting in Cu⁺ and Cu²⁺O⁻ sites⁶⁹ or a bridged binuclear Cu²⁺ site. In the latter case, desorption of O₂ gives two Cu⁺

sites.⁷⁰ In Cu-FAU, the autoreduction was suggested to involve the formation of “[AlO]⁺” Lewis acid sites, as first described by Jacobs and Beyer,⁷¹ although the former process was also suggested. This autoreduction for Cu zeolites is confirmed by XAFS spectroscopy, showing a reduction of the number of O atoms constituting the first coordination shell and the observation of a feature at 8983 eV in the XANES spectra,⁷² assigned as the 1s → 4p transition in Cu⁺.⁷³ In addition, monovalent Cu in MFI is characterized by two typical luminescence bands around 470–490 and 520–540 nm, assigned to transitions from the 3d⁹4s¹ triplet state to the 3d¹⁰ singlet ground state.^{74–76}

(64) Heijboer, W. M.; Battiston, A. A.; Knop-Gericke, A.; Havecker, M.; Mayer, R.; Bluhm, H.; Schlogl, R.; Weckhuysen, B. M.; Koningsberger, D. C.; de Groot, F. M. F. *J. Phys. Chem. B* **2003**, *107*, 13069–13075.

(65) Battiston, A. A.; Bitter, J. H.; de Groot, F. M. F.; Overweg, A. R.; Stephan, O.; van Bokhoven, J. A.; Kooyman, P. J.; van der Spek, C.; Vanko, G.; Koningsberger, D. C. *J. Catal.* **2003**, *213*, 251–271.

(66) Marturano, P.; Drozdova, L.; Pirngruber, G. D.; Kogelbauer, A.; Prins, R. *Phys. Chem. Chem. Phys.* **2001**, *3*, 5585–5595.

(67) Heijboer, W. M.; Battiston, A. A.; Knop-Gericke, A.; Havecker, M.; Bluhm, H.; Weckhuysen, B. M.; Koningsberger, D. C.; de Groot, F. M. F. *Phys. Chem. Chem. Phys.* **2003**, *5*, 4484–4491.

(68) Garten, R. L.; Delgass, W. N.; Boudart, M. *J. Catal.* **1970**, *18*, 90–107.

(69) Larsen, S. C.; Aylor, A.; Bell, A. T.; Reimer, J. A. *J. Phys. Chem.* **1994**, *98*, 11533–11540.

(70) Iwamoto, M.; Yahiro, H.; Tanda, K.; Mizuno, N.; Mine, Y.; Kagawa, S. *J. Phys. Chem.* **1991**, *95*, 3727–3730.

(71) Jacobs, P. A.; Beyer, H. K. *J. Phys. Chem.* **1979**, *83*, 1174–1177.

(72) Groothaert, M. H.; van Bokhoven, J. A.; Battiston, A. A.; Weckhuysen, B. M.; Schoonheydt, R. A. *J. Am. Chem. Soc.* **2003**, *125*, 7629–7640.

(73) Kau, L. S.; Spirasolomon, D. J.; Pennerhahn, J. E.; Hodgson, K. O.; Solomon, E. I. *J. Am. Chem. Soc.* **1987**, *109*, 6433–6442.

(74) Nachtigallova, D.; Nachtigall, P.; Sierka, M.; Sauer, J. *Phys. Chem. Chem. Phys.* **1999**, *1*, 2019–2026.

(75) Nachtigall, P.; Nachtigallova, D.; Sauer, J. *J. Phys. Chem. B* **2000**, *104*, 1738–1745.

(76) Nachtigallova, D.; Nachtigall, P.; Sauer, J. *Phys. Chem. Chem. Phys.* **2001**, *3*, 1552–1559.

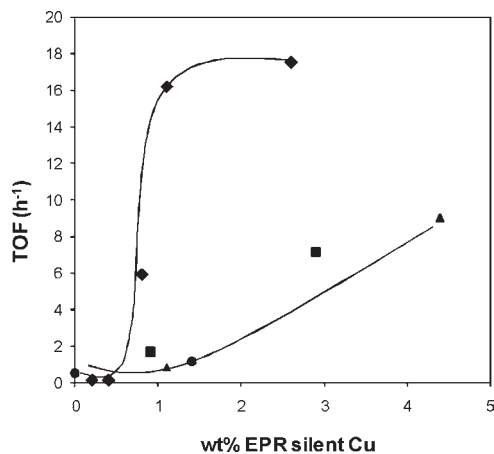


Figure 5. Activity per Cu (TOF) for N_2O decomposition as a function of the EPR-silent Cu^{2+} in (◆) Cu-ZSM-5 (Si/Al = 12), (▲) Cu-MOR (Si/Al = 8.8), (●) Cu-BEA (Si/Al = 9.8), and (■) Cu-FER (Si/Al = 6.2). Reprinted from ref 80 with permission from Elsevier 2007.

The 480 nm band is assigned to Cu^+ coordinated to three or four O atoms of the 6MR in the sinusoidal channels of ZSM-5. The 540 nm emission is attributed to Cu^+ coordinated to two O atoms at channel intersections. As for Cu^{2+} , the preferred O atoms in the coordination sphere of Cu^+ are those of the Si–O–Al bridges. What is still unclear is whether the sites of Cu^+ are the same as those of Cu^{2+} , in other words, whether or not the reduction of divalent Cu is accompanied by the migration of Cu^+ to a new coordination site.

4. Activated O_2 on TMI and Its Reactivity

4.1. Cu Zeolites. Autoreduction is a crucial step in the catalytic decomposition of NO and N_2O into N_2 and O_2 over Cu zeolite catalysts. Indeed, the O atoms of N_2O and NO are deposited on Cu^+ with the release of N_2 and N_2O , respectively. In the rate-limiting step, these deposited O atoms recombine and desorb as molecular oxygen.^{29,72,77–80} The closer the deposited O species are located to each other, the faster is the recombination. This is shown in Figure 5 for the N_2O decomposition over a range of Cu-exchanged zeolites. Here the amount of EPR-silent Cu^{2+} is used as a measure of the average Cu–Cu distance because Cu^{2+} becomes EPR-inactive as a result of antiferromagnetic coupling or dipolar broadening between closely located Cu^{2+} cores. A smooth increase of the N_2O decomposition activity with the amount of EPR-silent Cu has been observed in MOR, ferrierite (FER), and BEA catalysts.⁸⁰ Notably, Cu-ZSM-5 shows a much higher activity for decomposing N_2O , as can be seen in Figure 5. Clearly, a special type of active site must be present in ZSM-5. A similar trend was observed in the decomposition of NO. Cu-rich ZSM-5 samples (with Cu/Al > 0.2) show much higher activity compared to other Cu zeolites. In the work of Schoonheydt and co-workers, this was attributed to the presence of a unique Cu core with a characteristic absorption feature around $22\,700\text{ cm}^{-1}$, which was detected by in situ UV–vis absorption spectroscopy during catalytic decomposition of NO and N_2O .^{77,80}

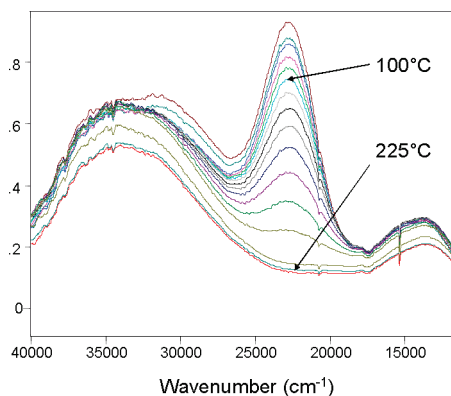


Figure 6. Fiber-optic UV–vis spectra of an O_2 -calced ($450\text{ }^\circ\text{C}$) Cu-ZSM-5 (Si/Al = 12; Cu/Al = 0.54) during reaction with CH_4 at a heating rate of $10\text{ }^\circ\text{C}/\text{min}$ from room temperature up to $225\text{ }^\circ\text{C}$. The time interval between two spectra is 1.5 min or a temperature difference of $15\text{ }^\circ\text{C}$. Reprinted from ref 82 with permission from Elsevier 2005.

Interestingly, a similar absorption band was also observed after contact of Cu-ZSM-5 catalysts with high Cu/Al ratios (Cu/Al > 0.25) with O_2 at elevated temperatures.^{72,81} Because O_2 is consumed in the process, the unique absorption may tentatively be assigned to an O-activated Cu species. Moreover, the active oxygen was found to selectively oxidize methane into methanol in a stoichiometric reaction, starting at $100\text{ }^\circ\text{C}$ (Figure 6).^{81,82} During the reaction with CH_4 , the $22\,700\text{ cm}^{-1}$ band disappears, indicating that the active Cu core in ZSM-5 is involved in both the catalytic decomposition of nitrogen oxides and the selective oxidation of methane.^{77,80} The nature of the active Cu core was investigated in a combined UV–vis, EPR, and EXAFS study, and the obtained data were suggested to be consistent with a bis-(μ -oxo)dicopper(III) core.^{72,77} The energy of the absorption band and the Cu–Cu distance of 2.87 \AA obtained by EXAFS were used to rule out the presence of a peroxo moiety, which typically has longer Cu–Cu distances.⁸³ From the amount of methanol produced, the number of active Cu centers was estimated to be approximately 5% of the total amount of Cu in Cu-ZSM-5; i.e., the species associated with $22\,700\text{ cm}^{-1}$ is a minority species.^{81,82} As EXAFS shows the averaged data for all Cu sites in Cu-ZSM-5, it is not sensitive enough to probe these active Cu sites. Because several Cu–O species show absorption features in this region,^{84–90} no conclusive assignment can

(81) Groothaert, M. H.; Smeets, P. J.; Sels, B. F.; Jacobs, P. A.; Schoonheydt, R. A. *J. Am. Chem. Soc.* **2005**, *127*, 1394–1395.

(82) Smeets, P. J.; Groothaert, M. H.; Schoonheydt, R. A. *Catal. Today* **2005**, *110*, 303–309.

(83) Tyeklar, Z.; Jacobson, R. R.; Wei, N.; Murthy, N. N.; Zubieta, J.; Karlin, K. D. *J. Am. Chem. Soc.* **1993**, *115*, 2677–2689.

(84) Baldwin, M. J.; Ross, P. K.; Pate, J. E.; Tyeklar, Z.; Karlin, K. D.; Solomon, E. I. *J. Am. Chem. Soc.* **1991**, *113*, 8671–8679.

(85) Baldwin, M. J.; Root, D. E.; Pate, J. E.; Fujisawa, K.; Kitajima, N.; Solomon, E. I. *J. Am. Chem. Soc.* **1992**, *114*, 10421–10431.

(86) Mahapatra, S.; Halfen, J. A.; Wilkinson, E. C.; Pan, G. F.; Cramer, C. J.; Que, L.; Tolman, W. B. *J. Am. Chem. Soc.* **1995**, *117*, 8865–8866.

(87) Root, D. E.; Mahroof-Tahir, M.; Karlin, K. D.; Solomon, E. I. *Inorg. Chem.* **1998**, *37*, 4838–4848.

(88) Chen, P.; Fujisawa, K.; Solomon, E. I. *J. Am. Chem. Soc.* **2000**, *122*, 10177–10193.

(89) Chen, P.; Root, D. E.; Campochiaro, C.; Fujisawa, K.; Solomon, E. I. *J. Am. Chem. Soc.* **2003**, *125*, 466–474.

(90) Maiti, D.; Fry, H. C.; Woertink, J. S.; Vance, M. A.; Solomon, E. I.; Karlin, K. D. *J. Am. Chem. Soc.* **2007**, *129*, 264–265.

(77) Groothaert, M. H.; Lievens, K.; Leeman, H.; Weckhuysen, B. M.; Schoonheydt, R. A. *J. Catal.* **2003**, *220*, 500–512.

(78) Dandekar, A.; Vannice, M. A. *Appl. Catal., B* **1999**, *22*, 179–200.

(79) Kapteijn, F.; Marban, G.; Rodriguez Mirasol, J.; Moulijn, J. A. *J. Catal.* **1997**, *167*, 256–265.

(80) Smeets, P. J.; Groothaert, M. H.; van Teeffelen, R. M.; Leeman, H.; Hensen, E. J. M.; Schoonheydt, R. A. *J. Catal.* **2007**, *245*, 358–368.

be made based on the UV-vis electronic absorption data alone.

Several density functional theory studies evaluated the possible binuclear Cu species formed in Cu-ZSM-5 upon calcination in O₂. From the calculations of Yumura et al., both side-on peroxo and bis(μ -oxo)dicopper cores were found to be energetically favorable in the 10MR of ZSM-5.⁹¹ In the work of Goodman et al. and Bell and co-workers, several oxygen-bridged binuclear Cu sites were proposed.^{92–94} In the work of Iwamoto et al.,⁹⁵ and later others,^{96–100} an oxygen-bridged Cu dimer was suggested to be formed during the auto-reduction of two hydrated Cu²⁺ cores. Aside from a Cu-Cu contribution in EXAFS data, no other spectroscopic evidence for such a core with bridging oxygen was presented to support the assignment. Computational studies have evaluated several possible core structures. Direct spectroscopic data are required that can selectively probe the active site, even if it is only a minority species. In fact, we have recently used the 22 700 cm⁻¹ absorption band to resonance enhance the Raman vibrations of the catalytic site upon shooting a laser in this absorption band. In these studies, the reactive intermediate is unambiguously defined as a bent [Cu-O-Cu]²⁺ core, a species not previously observed in Cu/O₂ chemistry, as the catalytically active species. The details of these spectroscopic studies and the frontier orbitals involved in H-atom abstraction from CH₄ are presented in ref 101.

In addition to this Cu core in Cu-ZSM-5, other Cu sites are capable of stoichiometric oxidation of methane in methanol.⁸² In Cu-MOR, a similar absorption feature at 22 000 cm⁻¹ was observed after O₂ calcination, although much less intense than that of Cu-ZSM-5. This band also disappeared during reaction with CH₄ at 150 °C, and methanol was produced. Less active Cu cores were formed in FER and BEA. Here, a reaction temperature of 200 °C is required to convert methane into methanol. In MOR, the amount of methanol produced after reaction at 200 °C significantly increased, compared to the reaction at 150 °C, indicating the presence of an additional core. Thus, while an activated Cu species, corresponding to the 22 700 cm⁻¹ absorption band in ZSM-5

and MOR, is capable of oxidizing CH₄ at 100 °C, another less active but unknown Cu species is present in the FER, BEA, and MOR zeolites that is capable of only oxidizing methane above 200 °C.⁸²

4.2. Fe Zeolites. Panov and co-workers reported the formation of the so-called α -O core in Fe-ZSM-5 upon reacting the zeolite with N₂O,^{102–104} suggested to mimic the selective hydroxylation of methane into methanol by the enzyme sMMO.^{105–107} High-temperature treatment in He, vacuum, H₂, or steam generates the precursor for this α -O core and is referred to as α -Fe.^{108–113} Subsequent reaction of the Fe zeolite with N₂O at temperatures between 200 and 250 °C results in the formation of α -O, a site capable of selectively oxidizing methane to methanol and benzene to phenol at room temperature. There is a consensus that this active site cannot be formed with O₂.^{114–116} Several studies address the comparison and differences between α -O and the active site in sMMO.^{61,110,117,118} In the past decades, a number of structural assignments, often contradictory, have been made for the α -O and α -Fe sites, and no consensus as to its structure has been attained thus far. Part of the controversy is due to the lack of a direct correlation between the reported spectroscopic data and the reactivity of these sites in the oxidation of CH₄ or benzene. On the basis of Mössbauer spectroscopy and EXAFS data, the core was originally assigned to a bis(μ -oxo)diiron core, in analogy with the active site in sMMO.¹⁰⁷ Later work suggested the formation of a Fe⁴⁺=O intermediate^{61,119} or alternatively a Fe³⁺O^{•-} radical^{120,121} or two Fe³⁺O^{•-} μ -OH-bridged sites.¹¹³ The formation of an Fe³⁺O^{•-} radical was tentatively suggested, based on the coexistence of signals at $g = 6.4$ and 2.018 in the EPR spectrum, assigned to Fe³⁺ and an

- (91) Yumura, T.; Takeuchi, M.; Kobayashi, H.; Kuroda, Y. *Inorg. Chem.* **2009**, *48*, 508–517.
 (92) Rice, M. J.; Chakraborty, A. K.; Bell, A. T. *J. Phys. Chem. B* **2000**, *104*, 9987–9992.
 (93) Goodman, B. R.; Schneider, W. F.; Hass, K. C.; Adams, J. B. *Catal. Lett.* **1998**, *56*, 183–188.
 (94) Goodman, B. R.; Hass, K. C.; Schneider, W. F.; Adams, J. B. *J. Phys. Chem. B* **1999**, *103*, 10452–10460.
 (95) Iwamoto, M.; Furukawa, H.; Mine, Y.; Uemura, F.; Mikuriya, S. I.; Kagawa, S. *J. Chem. Soc., Chem. Commun.* **1986**, 1272–1273.
 (96) Sarkany, J.; Ditri, J. L.; Sachtler, W. M. H. *Catal. Lett.* **1992**, *16*, 241–249.
 (97) Da Costa, P.; Moden, B.; Meitzner, G. D.; Lee, D. K.; Iglesia, E. *Phys. Chem. Chem. Phys.* **2002**, *4*, 4590–4601.
 (98) Palomino, G. T.; Fiscaro, P.; Bordiga, S.; Zecchina, A.; Giamello, E.; Lamberti, C. *J. Phys. Chem. B* **2000**, *104*, 4064–4073.
 (99) Xamena, F.; Fiscaro, P.; Berlier, G.; Zecchina, A.; Palomino, G. T.; Prestipino, C.; Bordiga, S.; Giamello, E.; Lamberti, C. *J. Phys. Chem. B* **2003**, *107*, 7036–7044.
 (100) Grunert, W.; Hayes, N. W.; Joyner, R. W.; Shpiro, E. S.; Siddiqui, M. R. H.; Baeva, G. N. *J. Phys. Chem.* **1994**, *98*, 10832–10846.
 (101) Woertink, J. S.; Smeets, P. J.; Groothaert, M. H.; Vance, M. A.; Sels, B. F.; Schoonheydt, R. A.; Solomon, E. I. *Proc. Natl. Acad. Sci. U.S.A.* **2009**, *106*, 18908–18913.

- (102) Panov, G. I.; Sobolev, V. I.; Kharitonov, A. S. *J. Mol. Catal.* **1990**, *61*, 85–97.
 (103) Panov, G. I.; Sheveleva, G. A.; Kharitonov, A. S.; Romannikov, V. N.; Vostrikova, L. A. *Appl. Catal., A* **1992**, *82*, 31–36.
 (104) Sobolev, V. I.; Kharitonov, A. S.; Paukshtis, Y. A.; Panov, G. I. *J. Mol. Catal.* **1993**, *84*, 117–124.
 (105) Dubkov, K. A.; Sobolev, V. I.; Talsi, E. P.; Rodkin, M. A.; Watkins, N. H.; Shteinman, A. A.; Panov, G. I. *J. Mol. Catal. A* **1997**, *123*, 155–161.
 (106) Dubkov, K. A.; Sobolev, V. I.; Panov, G. I. *Kinet. Catal.* **1998**, *39*, 72–79.
 (107) Ovanesyan, N. S.; Shteinman, A. A.; Dubkov, K. A.; Sobolev, V. I.; Panov, G. I. *Kinet. Catal.* **1998**, *39*, 792–797.
 (108) Kubanek, P.; Wichterlova, B.; Sobalik, Z. *J. Catal.* **2002**, *211*, 109–118.
 (109) Ribera, A.; Arends, I.; de Vries, S.; Perez-Ramirez, J.; Sheldon, R. A. *J. Catal.* **2000**, *195*, 287–297.
 (110) Knops-Gerrits, P. P.; Goddard, W. A. *J. Mol. Catal. A* **2001**, *166*, 135–145.
 (111) Hensen, E. J. M.; Zhu, Q.; Hendrix, M.; Overweg, A. R.; Kooyman, P. J.; Sychev, M. V.; van Santen, R. A. *J. Catal.* **2004**, *221*, 560–574.
 (112) Sun, K. Q.; Zhang, H. D.; Xia, H.; Lian, Y. X.; Li, Y.; Feng, Z. C.; Ying, P. L.; Li, C. *Chem. Commun.* **2004**, 2480–2481.
 (113) Dubkov, K. A.; Ovanesyan, N. S.; Shteinman, A. A.; Starokon, E. V.; Panov, G. I. *J. Catal.* **2002**, *207*, 341–352.
 (114) Ivanov, A. A.; Chernyavsky, V. S.; Gross, M. J.; Kharitonov, A. S.; Uriarte, A. K.; Panov, G. I. *Appl. Catal., A* **2003**, *249*, 327–343.
 (115) Yuranov, I.; Bulushev, D. A.; Renken, A.; Kiwi-Minsker, L. *J. Catal.* **2004**, *227*, 138–147.
 (116) Roy, P. K.; Pirngruber, G. D. *J. Catal.* **2004**, *227*, 164–174.
 (117) Ovanesyan, N. S.; Sobolev, V. I.; Dubkov, K. A.; Panov, G. I.; Shteinman, A. A. *Russ. Chem. Bull.* **1996**, *45*, 1509–1510.
 (118) Shilov, A. E.; Shteinman, A. A. *Acc. Chem. Res.* **1999**, *32*, 763–771.
 (119) Jia, J. F.; Sun, Q.; Wen, B.; Chen, L. X.; Sachtler, W. M. H. *Catal. Lett.* **2002**, *82*, 7–11.
 (120) Pirngruber, G. D.; Grunwaldt, J. D.; van Bokhoven, J. A.; Kalytta, A.; Reller, A.; Safonova, O. V.; Glatzel, P. *J. Phys. Chem. B* **2006**, *110*, 18104–18107.
 (121) Pirngruber, G. D.; Grunwaldt, J. D.; Roy, P. K.; van Bokhoven, J. A.; Safonova, O.; Glatzel, P. *Catal. Today* **2007**, *126*, 127–134.

$O^{\cdot-}$ radical moiety, respectively.¹²² However, if an $Fe^{3+}O^{\cdot-}$ core exists, $S = 5/2$ of Fe^{3+} should couple antiferromagnetically with the radical $S = 1/2$, resulting in an overall $S = 2$ ground state, which would not be detectable by X-band EPR spectroscopy at liquid- N_2 temperatures.^{123–125} $Fe^{4+}=O$ was ruled out because it would not contribute to the EPR spectrum at liquid- N_2 temperatures. However, the total amount of spin observed was not quantified with respect to the total Fe content. Thus, it is not possible to judge whether the presence of EPR-silent Fe centers, such as $Fe^{4+}=O$, can be excluded. Assignment of these EPR features to the active site was based on their disappearance after interaction with CO at room temperature, but the more direct approach of measuring the EPR spectra after reaction with CH_4 was not pursued. In combination with the above-mentioned EPR study, X-ray absorption data were collected and presented as inconsistent with an Fe^{4+} species.^{120,121,126} However, these bulk techniques do not rule out the presence of a minor amount of catalytic Fe^{4+} in the presence of a large fraction of spectator sites. Thus, no data exist that can unambiguously evaluate for the presence or absence of an Fe^{4+} core or relate it to the reactive α -O species. Recently, attempts have been undertaken to investigate the α -O site with UV–vis absorption and resonance Raman spectroscopy by Li and co-workers,¹²⁷ and the α site was tentatively assigned as a peroxo-bridged binuclear Fe site, based on the observation of a stretch at 867 cm^{-1} and an electronic absorption band at 605 nm ($16\,500\text{ cm}^{-1}$).

The formation of this α -O and the subsequent hydroxylation of CH_4 and benzene could only be achieved after deposition of an O atom from N_2O but not after reaction with O_2 . The treatment of Fe-ZSM-5 with O_2 was studied in the work of Sachtler and co-workers.¹²⁸ In their Raman study, an adsorbed peroxide species was suggested to be formed, bridging two Fe^{3+} centers. The presence of a peroxo intermediate was concluded based on a Raman feature at 730 cm^{-1} assigned as the O–O stretching vibration. Distinguishing vibrations involving O motions can be made upon ^{18}O isotopic labeling because these vibrations shift to lower frequencies. The work of Sachtler and co-workers shows a red shift of 32 to 698 cm^{-1} when Fe-ZSM-5 is treated with $^{18}O_2$, confirming the involvement of extralattice O motion in the Fe complex. In Fe zeolites, the presence of Fe dimers is suggested to be reflected by the presence of an absorption band in the $28\,000$ – $30\,000\text{ cm}^{-1}$ region,¹²⁹ but this assignment is debated.¹²⁶ Interestingly, however, a peroxo-bridged Fe^{3+} dimer is suggested in the work of Sachtler as well

as in the work of Li and co-workers, although the suggested peroxo stretches at 730 and 867 cm^{-1} are very different.^{127,128} More detailed spectroscopic investigation is thus required to further unravel the geometric and electronic structures of the O-bridged Fe dimers suggested to be formed from O_2 and N_2O . If it is, in fact, the case that both N_2O and O_2 treatments result in peroxo-bridged Fe dimers, as suggested by Li and Sachtler, respectively, it is important to understand how the different geometric and electronic structures (resulting in different peroxo stretches) contribute to their different reactivities. Only the N_2O -activated form, α -O (which is not formed with O_2), is active in the selective oxidation of CH_4 and benzene at room temperature.

O_2 treatment of Fe zeolites does not result in the formation of active sites for the selective oxidation of methane and benzene. Rather, activated O_2 species in Fe zeolites catalyze the nonselective oxidation of hydrocarbons into CO_x and H_2O at elevated temperatures (typically at $400\text{ }^\circ\text{C}$ or higher). This is observed in the selective catalytic reduction (SCR) of NO (similar to that in Cu and Co zeolites). At moderate temperatures (typically between 250 and $350\text{ }^\circ\text{C}$), O_2 is beneficial for the SCR of NO. O_2 and activated O_2 species have been suggested to (i) oxidize NO into NO_2 or adsorbed NO_y (with $y = 2, 3$) species, (ii) reoxidize the TMI to its “proper” oxidation state for NO– NO_2 conversion and adsorption,^{130–136} (iii) remove carbonaceous deposits,¹³⁷ and (iv) oxidize hydrocarbons into more reactive oxygenated surface intermediates for NO reduction.¹³⁸ At higher temperatures, however, the presence of O_2 results in a decreased reduction of NO, resulting in the typically observed volcano-shaped conversion curves. The combustion of the hydrocarbons with the activated oxygen species is more dominant at these temperatures, leaving fewer hydrocarbons for the reduction of NO_x .^{40,139,140} Little is known, however, on the geometric and electronic structures of the intermediates involved in both the low- and high-temperature reactions.

4.3. Co and Other First-Row TMI Zeolites. Other first-row TMIs, such as Ti, V, Cr, and Mn, have been reported to be active in either N_2O decomposition or selective oxidation reactions. Recently, the presence of an α -O site in Mn-ZSM-5 was suggested after N_2O treatment, similar to Fe-ZSM-5. This so-called α -O results in the formation of an absorption band in the UV–vis spectra around $18\,500\text{ cm}^{-1}$ and was suggested to be involved in the N_2O

(122) Berrier, E.; Ovsitser, O.; Kondratenko, E. V.; Schwidder, M.; Grunert, W.; Bruckner, A. *J. Catal.* **2007**, *249*, 67–78.

(123) Neidig, M. L.; Decker, A.; Choroba, O. W.; Huang, F.; Kavana, M.; Moran, G. R.; Spencer, J. B.; Solomon, E. I. *Proc. Natl. Acad. Sci. U.S.A.* **2006**, *103*, 12966–12973.

(124) Solomon, E. I.; Wong, S. D.; Liu, L. V.; Decker, A.; Chow, M. S. *Curr. Opin. Chem. Biol.* **2009**, *13*, 99–113.

(125) Krzystek, J.; England, J.; Ray, K.; Ozarowski, A.; Smirnov, D.; Que, L.; Telsler, J. *Inorg. Chem.* **2008**, *47*, 3483–3485.

(126) Pirngruber, G. D.; Roy, P. K.; Prins, R. *Phys. Chem. Chem. Phys.* **2006**, *8*, 3939–3950.

(127) Xia, H. A.; Sun, K. Q.; Sun, K. J.; Feng, Z. C.; Li, W. X.; Li, C. *J. Phys. Chem. C* **2008**, *112*, 9001–9005.

(128) Gao, Z. X.; Kim, H. S.; Sun, Q.; Stair, P. C.; Sachtler, W. M. H. *J. Phys. Chem. B* **2001**, *105*, 6186–6190.

(129) Capek, L.; Kreibich, V.; Dedecek, J.; Grygar, T.; Wichterlova, B.; Sobalik, Z.; Martens, J. A.; Brosius, R.; Tokarova, V. *Microporous Mesoporous Mater.* **2005**, *80*, 279–289.

(130) Hamada, H.; Kintaichi, Y.; Sasaki, M.; Ito, T.; Tabata, M. *Appl. Catal.* **1991**, *70*, L15–L20.

(131) Komatsu, T.; Nunokawa, M.; Moon, I. S.; Takahara, T.; Namba, S.; Yashima, T. *J. Catal.* **1994**, *148*, 427–437.

(132) Ham, S. W.; Choi, H.; Nam, I. S.; Kim, Y. G. *Catal. Lett.* **1996**, *42*, 35–40.

(133) Eng, J.; Bartholomew, C. H. *J. Catal.* **1997**, *171*, 27–44.

(134) Schay, Z.; James, V. S.; Pal-Borbely, G.; Beck, A.; Ramaswamy, A. V.; Guzzi, L. *J. Mol. Catal. A* **2000**, *162*, 191–198.

(135) Delahay, R.; Kieger, S.; Tanchoux, N.; Trens, P.; Coq, B. *Appl. Catal., B* **2004**, *52*, 251–257.

(136) Sjoval, H.; Olsson, L.; Fridell, E.; Blint, R. J. *Appl. Catal., B* **2006**, *64*, 180–188.

(137) d'Itri, J. L.; Sachtler, W. M. H. *Appl. Catal., B* **1993**, *2*, L7–L15.

(138) Montreuil, C. N.; Shelef, M. *Appl. Catal., B* **1992**, *1*, L1–L8.

(139) Chen, H. Y.; Voskoboinikov, T.; Sachtler, W. M. H. *J. Catal.* **1999**, *186*, 91–99.

(140) Parvulescu, V. I.; Grange, P.; Delmon, B. *Catal. Today* **1998**, *46*, 233–316.

decomposition in Mn-ZSM-5.¹⁴¹ No reactivity toward hydrocarbons is thus far reported for this species, and as is the case for Fe-ZSM-5, the α -O in Mn-ZSM-5 cannot be formed with O₂. Although Mn zeolites have been reported to catalyze the selective oxidation of *n*-hexane with O₂, the role of the Mn sites is not in O₂ activation. The proposed role of Mn is rather to regulate the selective decomposition of the hexylhydroperoxo intermediate in this reaction.¹⁴² Isomorphously substituted V, Cr, and Ti zeolites and mesoporous materials were found to be active in the photocatalytic partial oxidation of hydrocarbons with O₂.^{143,144} Supported isolated vanadium oxides on SiO₂, TiO₂, Al₂O₃, or mesoporous materials are often investigated in the selective oxidation of CH₄ or methanol into formaldehyde with O₂ at temperatures above 400 °C.^{145–151} Isomorphous substitution of Ti in the zeolite lattice, e.g., TS-1 zeolite, results in active catalysts for the liquid-phase catalytic oxidation of a variety of organic compounds with H₂O₂.

Co-exchanged zeolites or Co incorporated in the lattice of AlPO's has often been reported to be active in the selective oxidation of linear alkanes by O₂.^{152,153} Co-exchanged X and Y zeolites or the mesoporous silica MCM-41 has been found to be active in the epoxidation of styrene with molecular oxygen in the presence of *N,N*-dimethylformamide (DMF).^{154–156} A tentative reaction mechanism was proposed for the O₂ oxidation of α -pinene and the epoxidation of styrene by Co-exchanged FAU.^{155,157} Activation of O₂ in the presence of DMF at the Co sites is suggested to occur via a tetrahedrally coordinated cobalt(III) superoxo complex, with a typical absorption band at 620 nm (16 130 cm⁻¹) in the UV–vis absorption spectrum,¹⁵⁵ followed by oxidative addition to the C=C double bond of styrene and α -pinene.

5. Conclusions

This Forum contribution has reviewed the coordination of Cu²⁺, Fe³⁺, and Co²⁺ to surface O atoms in zeolites, as derived from spectroscopic and theoretical studies, the

formation of activated oxygen species, and their role in selective oxidation reactions. At low loadings, the coordination of the TMI is reasonably well understood. Cu²⁺ is found to coordinate in 6MR, distorting the ring in such a way as to obtain 4-fold coordination. In the case of Co²⁺, it can have 3–5-fold coordination. The resulting site distortion depends on the amount of Al tetrahedra making up that site. Thus, a TMI in one crystallographic exchange site can have several spectroscopic signatures, depending on the number of Al tetrahedra. As a result, both the crystallographic position of the exchange site and the number of Al tetrahedra making up the site determine the spectroscopic signature and thus the geometric and electronic structures of the TMI in that site.

Increasing the TMI loading increases the heterogeneity of the TMI species formed at the zeolite surface. This can result in the formation of di- and oligomeric species requiring extralattice ligands (water, hydroxo, and oxo ligands). Removal of these ligands during high-temperature pretreatments can result in autoreduction of the TMI, as confirmed by XANES and UV–vis studies. Several mechanisms for autoreduction have been suggested. However, decisive spectroscopic evidence for the proposed intermediates is lacking.

The reduced TMI sites possess interesting properties. At room temperature, O₂ is only weakly adsorbed in most zeolites, but superoxo complexes have been reported to be formed with Cu⁺ and Cr²⁺ in zeolite A. High-temperature treatment in O₂ leads to the formation of a catalytically interesting core in Cu-ZSM-5, characterized by a distinct absorption band around 22 700 cm⁻¹. A recent resonance Raman study allowed assignment of this active site as a bent [Cu–O–Cu]²⁺ core.¹⁰¹ This species, corresponding to only about 5% of the total amount of Cu, is the crucial intermediate in both the direct decomposition of NO and N₂O and the selective oxidation of methane into methanol in a stoichiometric reaction. Other Cu zeolites, not containing this species, are also active in the selective oxidation of methane into methanol but at higher temperature. Research is now directed toward (i) further understanding the electronic and geometric structures and reactivity of the bent [Cu–O–Cu]²⁺ core in the O₂-activated Cu-ZSM-5, (ii) obtaining more information on active sites in other Cu zeolites, (iii) devising a catalytic cycle for the methane-to-methanol conversion with Cu and Fe zeolites, and (iv) increasing the number of active sites.

An activated oxygen species, called α -O, is formed in Fe-ZSM-5. There is a lot of speculation as to the nature of this α -O species. All involve mono- and binuclear Fe–O species. Its definitive spectroscopic characterization and assignment is also lacking. Consensus, however, does exist on its role in the selective oxidation of methane and benzene into methanol and phenol, respectively, at room temperature. The hydroxylation of benzene was converted in a catalytic system upon an increase in the reaction temperature, favoring the desorption of phenol. In the reaction with CH₄, increasing the temperature results in the decomposition of methanol into CO₂ and H₂O, as is the case in O₂-activated Cu-ZSM-5. In contrast to Cu-ZSM-5, however, this reactive α -O in Fe-ZSM-5 cannot be formed with O₂ (i.e., only with N₂O).

The treatment of Co-exchanged FAU with O₂ is suggested to result in the formation of a cobalt(III) superoxo complex in FAU zeolite based on an absorption band at 620 nm. This superoxo species is found to be active in the epoxidation of styrene and the oxidation of α -pinene. Additional

(141) Radu, D.; Glatzel, P.; Gloter, A.; Stephan, O.; Weckhuysen, B. M.; de Groot, F. M. F. *J. Phys. Chem. C* **2008**, *112*, 12409–12416.

(142) Zhan, B. Z.; Moden, B.; Dakka, J.; Santiesteban, J. G.; Iglesia, E. *J. Catal.* **2007**, *245*, 316–325.

(143) Anpo, M.; Kim, T. H.; Matsuoka, M. *Catal. Today* **2009**, *142*, 114–124.

(144) Hu, Y.; Wada, N.; Tsujimaru, K.; Anpo, M. *Catal. Today* **2007**, *120*, 139–144.

(145) Herman, R. G.; Sun, Q.; Shi, C. L.; Klier, K.; Wang, C. B.; Hu, H. C.; Wachs, I. E.; Bhasin, M. M. *Catal. Today* **1997**, *37*, 1–14.

(146) Bronkema, J. L.; Bell, A. T. *J. Phys. Chem. C* **2007**, *111*, 420–430.

(147) Berndt, H.; Martin, A.; Bruckner, A.; Schreier, E.; Muller, D.; Kosslick, H.; Wolf, G. U.; Lucke, B. *J. Catal.* **2000**, *191*, 384–400.

(148) Koranne, M. M.; Goodwin, J. G.; Marcelin, G. *J. Catal.* **1994**, *148*, 378–387.

(149) Parmaliana, A.; Arena, F. *J. Catal.* **1997**, *167*, 57–65.

(150) Baltés, M.; Cassiers, K.; Van Der Voort, P.; Weckhuysen, B. M.; Schoonheydt, R. A.; Vansant, E. F. *J. Catal.* **2001**, *197*, 160–171.

(151) Deo, G.; Wachs, I. E. *J. Catal.* **1994**, *146*, 323–334.

(152) Thomas, J. M.; Raja, R.; Sankar, G.; Bell, R. G. *Nature* **1999**, *398*, 227–230.

(153) Thomas, J. M. *Angew. Chem., Int. Ed.* **1999**, *38*, 3589–3628.

(154) Tang, Q. H.; Wang, Y.; Liang, J.; Wang, P.; Zhang, Q. H.; Wan, H. L. *Chem. Commun.* **2004**, 440–441.

(155) Sebastian, J.; Jinka, K. M.; Jasra, R. V. *J. Catal.* **2006**, *244*, 208–218.

(156) Tang, Q. H.; Zhang, Q. H.; Wu, H. L.; Wang, Y. *J. Catal.* **2005**, *230*, 384–397.

(157) Patil, M. V.; Yadav, M. K.; Jasra, R. V. *J. Mol. Catal. A* **2007**, *277*, 72–80.

spectroscopic studies are needed to obtain insight into this O₂-formed active Co^{III} site and the molecular mechanism of these reactions.

Overall, O₂ activation depends on the interplay of structural factors such as the zeolite type and the size of the channels and cages and chemical factors such as the Si/Al ratio and nature, charge, and distribution of the cations. Spectroscopic techniques capable of selectively probing the active sites, even though they constitute only a minor fraction of the total amount of TMI sites, are thus required. The fundamental knowledge of the active site obtained from such

studies can provide detailed mechanistic insight and assist in the design and development of novel selective oxidation catalysts.

Acknowledgment. P.J.S. acknowledges IWT and KU Leuven for graduate and postdoctoral fellowships, and J.S.W. acknowledges the NIH for a traineeship. This research was supported by the GOA and the Long Term Structural Funding–Methusalem Funding by the Flemish Government (to R.A.S. and B.F.S.) and by NIH Grant DK-31450 (to E.I.S.).